Development of an Automated Feedback Loop for the Geometric Stabilization of Taylor Cones in Low Flow-Rate Magnetoelectrosprays

Patrick Gao

Development of an Automated Feedback Loop for the Geometric Stabilization of Taylor Cones in Low Flow-Rate Magnetoelectrosprays

Abstract

A Taylor cone is formed from a fluid meniscus subjected to an electric field, from which a stream of droplets, an electrospray, is ejected. Electrospray is widely applicable today, where the goal of spraying smaller and monodispersed droplets is strongly desirable for practical applications: cleaner readings in mass spectrometry and higher efficiency in satellite colloid thrusters. To achieve smaller monodispersed droplets, the stability of the Taylor cone must be maintained toward lower flow rates. The addition of a coincident magnetic field has also been shown to increase the stability of the Taylor cone. However, to control Taylor cones towards lower flow rates, a reliable method to control the geometry of the Taylor cone is needed. Therefore, the purpose of this study was to automate the method for Taylor cone angle control through a live image-processing program that detects and calculates the angle at the tip of a Taylor cone, and stabilizes the geometry through an Arduino interface with the electrospray. The angle-detection program was written and interfaced with the electrospray through an Arduino in order to record variable data over a range of decreasing flow rates. To judge the effectiveness of the cone-stabilization setup, Taylor cones were then geometrically stabilized at lower flow rates to observe the stabilizing effect of a coincident magnetic field. Preliminary data collected over a relatively narrow range of magnetic fields suggested a slight trend showing minimum flow rate converging towards lower values as the magnetic field increased. For all intents and purposes using the same methodology developed in this study, a more complete set of data was obtained subsequently by a researcher in the same laboratory. The subsequent dataset further supports the relationship between minimum flow rate and an applied magnetic field. In conjunction with the congregation of corresponding data points towards lower flow rates and voltages, the subsequent dataset suggests increased stability with an additional coincident magnetic field.

Development of an Automated Feedback Loop for the Geometric Stabilization of Taylor Cones in Low Flow-Rate Magnetoelectrosprays

Introduction

When a high voltage is applied across a liquid in a capillary relative to an electrode, electrostatic forces deform the meniscus formed at the tip, causing it to become unstable. At a threshold voltage where electrostatic forces are greater than forces exerted by the liquid and capillary, the meniscus forms into a Taylor cone in a state of electrohydrodynamic stability (Chen, 2011), characterized by an apex from which a cone-jet expels a stream of droplets (Cloupeau & Prunet-Foch, 1989) as shown in Figure 1. These droplets of uniform diameter typically smaller than 10 μm are radially dispersed due to Coulomb forces exerted between droplets, forming an electrospray. Droplets are formed as a result of Plateau-Rayleigh instability, in which a stream of liquid tends to separate into smaller droplets, as liquid droplets have a lower overall surface area than an unstable liquid column with the same volume. A larger air-liquid interface requires a higher amount of energy to maintain, therefore, a liquid stream experiencing varicose perturbations of increasing amplitude will break into droplets at each bulge, splitting at each pinch, upon reaching a critical diameter (Breslouer, 2010).

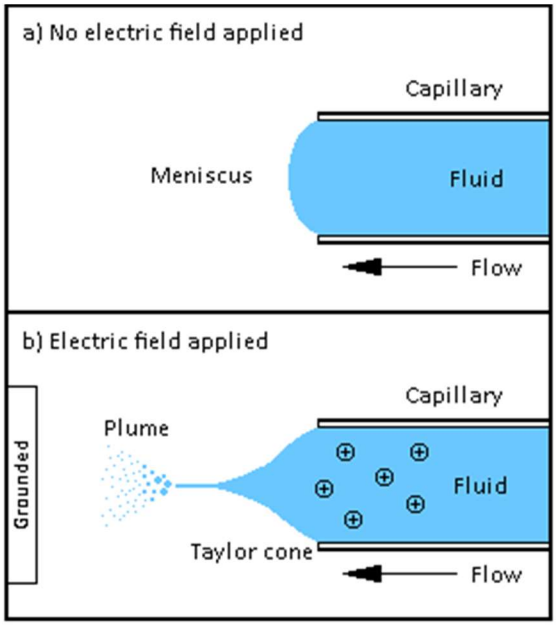

Figure 1. Taylor Cone. A Taylor cone is formed when an electric field is passed through a liquid in a capillary, where the meniscus (a) will extend outwards until past a critical voltage at which a jet stream will eject from the tip of the cone (b). Graphic by author.

The production of small droplets allows for the analysis of large macromolecules such as proteins through mass spectrometry without fragmentation (Ho *et al*., 2003). Alternatively, electrospray can similarly be used as one of the most efficient methods of rocket propulsion, used to adjust the position of satellites. The typical measure of propulsive efficiency, specific impulse, measures the generated thrust of a thruster per unit of propellant consumed. Electrospray has a significantly greater specific impulse than other conventional chemical or cold

gas methods (Roy *et al*., 2009), able to produce 10's of μN at a specific impulse of up to 3000s with less than 1 watt (Courtney, Dandavino, & Shea, 2002). Specific impulse (I_{sp}), calculated by Equation 1, is equal to the force of thrust [N] over the quantity of the flow rate (Q) of the propellant [kg/s] multiplied by standard gravity (g_0) given in [m/s^2].

$$I_{sp} = \frac{F_T}{g_0 \cdot Q} \qquad (1)$$

The resulting unit of specific impulse is simply in seconds, which is practical as seconds are used in both the metric and imperial systems. Despite the small scale at which electrospray operates, its high propulsive efficiency makes electrospray thrusters particularly suited for satellite control. Microgravity conditions allow electrospray thrusters to move relatively large objects with very little fuel, but many improvements can still be made to increase the power or efficiency at which they operate.

An electrospray can be modified by controlling a few variables: the electrical conductivity (K) and flow rate (Q) of the liquid pushed through the capillary, the voltage (V) across the spray, the current (I) of the charged liquid, and the surface tension (γ). Of these, Q, K, I, and γ affect the droplet size. Voltage, although having little effect on droplet size, must be within a (Q,V) stability window to maintain a cone, an area on the (Q,V) plane in which the cone remains stable. Flow rate, however, is important for achieving small drop sizes. At lower flow rates within the stability window, smaller drop sizes are produced (Fernandez de la Mora, 2007), increasing the charge per mass ratio and decreasing the needed voltage to achieve a certain specific impulse (Martinez-Sanchez & Lozano, 2015). Therefore, it is of practical importance to try to widen the stability window towards smaller flow rates, increasing the efficiency of electrospray thrusters for the use on satellites where any reduction in weight is highly desirable.

Magnetoelectrospray

In a previous study by King and his colleagues, increasing the output of an electrospray was achieved not through compounding methods such as a multiplexed electrospray (MES), in which multiple electrospray tips are arranged in an array (Lenguito, Fernandez de la Mora, & Gomez, 2010), but through exploiting the tendency for ferrofluids to form multiple tips in a magnetic field. Each ferrofluid tip would then be able to produce a spray, allowing multiple sprays from one emitter (King *et al*., 2006). The addition of a coincident magnetic field (B) has

been shown to decrease the electric field required to form a cone, reduced by up to 4.5×10^7 V/m (King *et al*., 2006). Furthermore, an additional magnetic field should hypothetically lead to more stable cones as a result of the combination of coincident electric and magnetic stresses, although the exact forces by which a magnetic field contributes to the stability of a magnetoelectrospray are still unclear.

Taylor Cone Geometry

Upon discovering the formation of a cone-jet when a drop is subjected to an electric field, G.I. Taylor calculated the theoretical half-angle of a conical interface, the angle between the altitude and the lateral side of a cone as shown in Figure 2, at equilibrium to be 49.3 degrees (Taylor, 1964). However, subsequent studies do not account for the geometry of the cone as much as the other controlling factors.

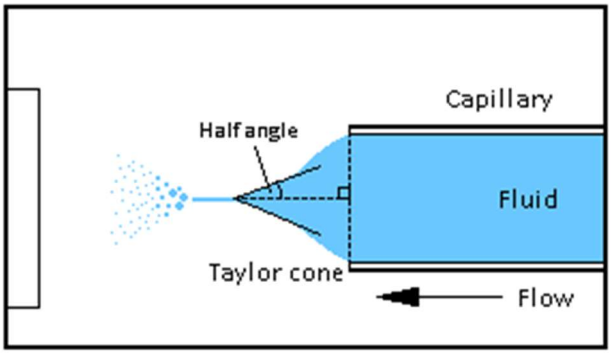

Figure 2. Half angle of a Taylor cone. The half angle calculated by G.I. Taylor, known as the Taylor angle, is the angle between the altitude and a lateral side of the cone. Graphic by author.

The ability to control for cone geometry is of significant importance, especially because the critical cone voltage is strongly geometrically dependent, as well as flow rate dependent. Therefore, in order to test for minimum flow rate, a method must be implemented to stabilize cone geometry through voltage. Current methods to measure the geometry of a Taylor cone are laborious and slow, one of which is achieved through physically measuring the angle of a Taylor cone with a protractor on a computer screen. The lack of automation and the absence of a feedback mechanism for angle control hinders the ability to collect large amounts of data efficiently. Therefore, the main purpose of this experiment was to attempt to automate the method for Taylor cone angle control through a live image-processing program that detects and calculates the angle at the tip of a Taylor cone, and stabilizes the geometry through an Arduino UNO interface with the electrospray. In addition, concerning the scientific interest of widening the (Q,V) stability window towards lower flow rates, the development of a Taylor cone stabilizing program leads to another goal of this experiment: to observe the effect of a coincident magnetic field on the stability of a magnetoelectrospray.

Engineering Considerations

With the development of a program written by the author that detects the angle formed at the apex of the Taylor cone and the implementation of a cone-stabilizing script, the cone geometry becomes a controlled variable. A significant portion of this study was spent creating this novel program from scratch, which consisted of several components to ultimately produce text records of several measured variables for analysis: angle-detection, PID control, and an Arduino UNO interface. PID, or proportional-integral-derivative, control was implemented into the angle-detection program to produce outputs for voltage to an Arduino UNO. This Arduino UNO served as the interface between the hardware and software, relaying values for voltage from the angle-detection program to the high-voltage power supply, while simultaneously reading values of pressure, voltage, and current for the electrospray and feeding them to the angle-detection program, as shown in Figure 3.

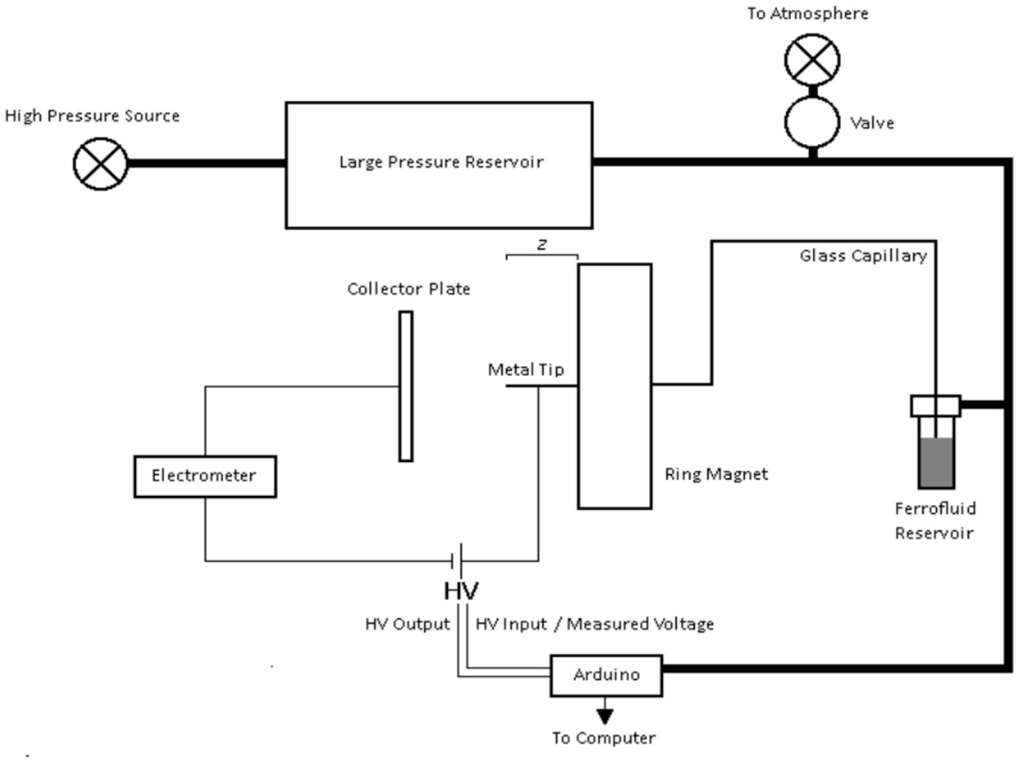

Figure 3. Electrospray setup. The electrospray was largely controlled through the Arduino, which served as the interface between the electrospray and the angle-detection program on a computer. A manually-controlled valve that extends between the pressure reservoir and the ferrofluid reservoir also serves as a source of controlled pressure loss within the ferrofluid vial that forces ferrofluid through the capillary and towards the metal tip centered in the ring magnet. The distance *z* is relevant in the equation to calculate the magnetic field at the end of the metal tip. The current of the high voltage (HV) circuit completed during an electrospray is measured with an electrometer connected in series, whereas the voltage is measured straight from the HV power source by the Arduino. Graphic by author.

In this setup, ferrofluid is pressurized in the vial with air from the large pressure reservoir and manually controlled using the valve, which forces ferrofluid through the glass capillary and therefore through the center of the ring magnet into the metal emitter tip. The ferrofluid is charged with positive ions through the emitter tip, which forms a Taylor cone that sprays ferrofluid towards the grounded collector plate, completing the high voltage circuit. The current is measured with an electrometer connected in series to the high voltage (HV) source, and the voltage is measured from the HV source through the Arduino UNO. The distance z between the metal emitter tip and the ring magnet shown in Figure 3 is later used to calculate the magnetic field at the emitter tip.

Angle Detection

The ability to measure the cone angle in real time was required to stabilize the cone geometry. Using Python 2.7 and the OpenCV 3.1.1 library, the findContours descriptor was used to find the edge of the Taylor cone. To produce a clean and defined edge prior to angle detection, a white background was used to contrast the black ferrofluid. The video capture, processed at a resolution of 1280 by 720 pixels at 60 frames per second, was then converted to grayscale and passed through a threshold to ensure a stark contrast at the edges. After this image refinement process, the findContours function is called and an array is produced containing all the points along the detected edges. The left-most point of this array was characterized as the vertex of the cone angle, while the intersections formed between a vertical line intersecting the cone contour served as the endpoints of the angle vectors. The angle was then calculated with the dot product of the two vectors drawn. The vertical line, or the angle base, position is set by the user depending on the position of the capillary tip in the capture frame, as shown in Figure 4.
For further insights into characteristics of the Taylor cone, a second angle called the tip angle was measured near the apex of the cone. For this angle, the corresponding intersecting vertical line was drawn a user-set pixel distance from the vertex of the cone angle, and therefore would move as the cone shape changed. A trackbar was later implemented to allow for the adjustment of the cone angle base in real-time.

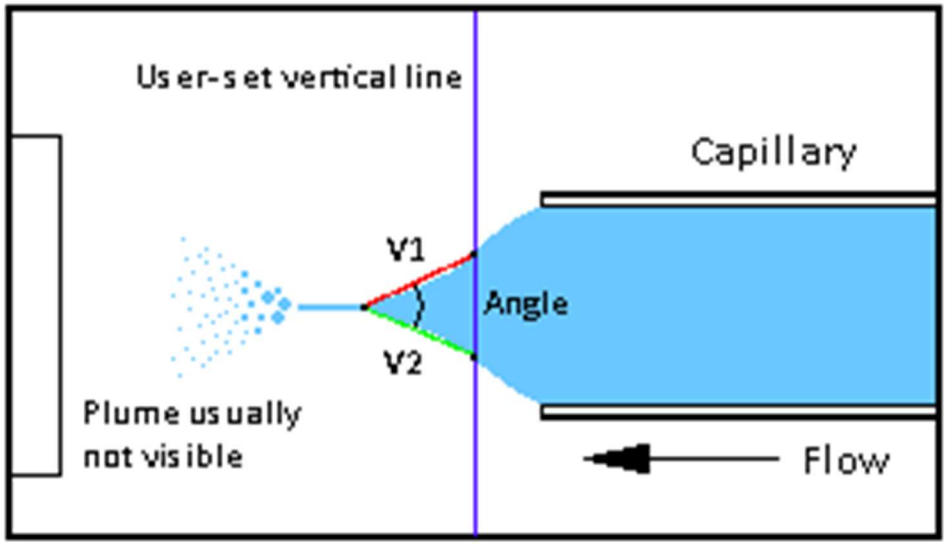

Figure 4. Angle-detection. The angle was calculated with the dot product of the two vectors: V1 (red), drawn from the vertex to one intersection of the vertical line (blue) and the cone contour, and V2 (green), drawn from the vertex to the other intersection of the vertical line (blue) and the cone contour. The vertical line is set by the user depending on the position of the capillary and cone relative to the camera frame. Graphic by author.

PID control

Now able to measure cone geometry, a PID controller was implemented to stabilize the cone angle. Using a standard Python PID control loop written by Durmusoglu (2010), the measured angle was input into the loop, producing a value corresponding to the direction and magnitude of change required to achieve the set point - which in this case was the desired angle. With the PID class called in the angle detection program, the output of the PID loop was added to the voltage output of the angle detection program, thereby adjusting the voltage of the electrospray as the cone geometry changes. The nature of the PID loop allows the PID output to be self-adjusting to the required voltage range, which was a 12-bit value corresponding to 0V - 5V in this experiment. The 0-5V range output by the Arduino UNO served as the input for the high voltage power source, which in turn output 0-5 kV. Through trial and error, the P-gain, I-gain, and D-gain values were set as 0.0008, 0.0, and 0.8, respectively. These values appeared to provide the most stable cone control compared to other combinations that were tested. Although attained without any concrete process or calculation, these gain values are reasonable for an electrospray system.

Before discussing gain values, several other terms must be understood. The error is the difference between the measured value and the desired value (set point), and an overshoot is when the measured value approaches the desired value but continues past it before returning. The P-gain, which determines the amount of change to the PID loop output due to a change in the

error (Hardy, 2010), should be relatively small (.0008) as the correct voltage should be achieved through a smooth curve with little overshoot rather than rapid oscillations with large overshoot that could be destructive to the stability of a Taylor cone, in the case of higher P-gain values. Having a zero I-gain is also reasonable as I-gain determines the amount to correct for the output over time due to changes in the error (Hardy, 2010), usually correcting for steady state error (Astrom, 2002). The dynamic nature of the electrospray system eliminates the need for this correction as there is no steady state error. Lastly, the D-gain controls how much to change the output in response to a change in direction of the error (Hardy, 2010). A value of 0.8 provides enough magnitude for the PID loop to respond to changes in geometry quickly enough to maintain stability, but also slowly enough to minimize oscillation. Another trackbar was also implemented for the adjustment of the set-point in real time, allowing multiple angles to be stabilized within one instance of the program.

Arduino UNO

An Arduino UNO was used to interface the angle detection program with the physical electrospray setup. Receiving values of pressure, voltage, and current from a MPX4250DP pressure sensor, the high-voltage power supply (BNC 3), and an electrometer (BNC 2), respectively, and two angle values for the cone angle from the base and from the tip (output from angle-detection program), the Arduino UNO printed all these variables to the angle detection program, as shown in Figure 5. After, a 12-bit output was enabled through the use of a MCP4725

Figure 5. Arduino UNO. The MPX4250DP pressure sensor from Freescale Semiconductor is mounted on top of the Arduino UNO while voltage and current are measured through BNC 3 and BNC 2 connectors, respectively. BNC 1 is for the HV input. Graphic by author.

digital-to-analog converter, and sent to the HV power supply to be converted to a voltage between 0-5 kV for the formation of a Taylor cone. Because of the serial nature of the Arduino UNO, the Arduino UNO program also written by the author in C can be characterized in a flow chart, described further in Figure 6. The angle detection program reads the incoming lines sent by the Arduino in the middle step, and records them to a text file for analysis. Reading and writing rates are therefore dependent on the rate at which the angle-detection program outputs a value to the Arduino UNO.

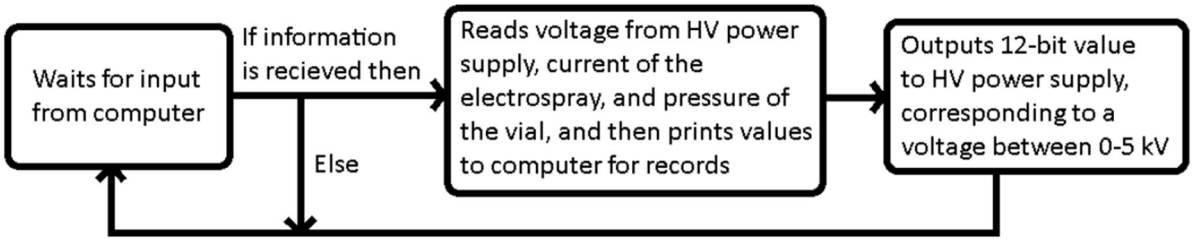

Figure 6. Arduino UNO loop. The Arduino UNO waits for a 12-bit input from the angle-detection program, after which, when received, the Arduino UNO will return readings for pressure, voltage, and current to the angle-detection program. It will then output a voltage between 0-5 V to the HV power supply, which is translated to 0-5 kV, and used to charge the liquid in electrospray. Graphic by author.

Data Sampling

As a parameter defined before beginning a video capture, the frame rate determines how often the angle-detection program should capture a still frame from the video camera. Each still frame was then put through the angle-detection process described previously, which includes the PID loop that outputs a 12-bit value for voltage to the Arduino UNO. Therefore, the overall data sampling rate was dependent on the frame rate of the video capture. In this experiment, a frame rate of 60 frames per second was used, although frame rates ranging from 120 fps to 10 fps were possible. The data sampling rate should therefore be sixty times per second, although the rate is probably lower in reality as a result of delays in serial communication between the computer and the Arduino UNO.

Methodology

The electrospray setup was constructed as depicted in Figure 3 previously. Most of the setup was pre-constructed, although the author did make minor repairs and adjustments for experimentation. The pressurized vial forces ferrofluid through the capillary, which is centered in

a rare-earth ring magnet with a 3 inch outer diameter, a 2 inch inner diameter, and a 0.5 inch width, and held in place with an upchurch fitting. The spray is charged through a metal emitter tip. The circuit is completed with a charged collector plate to receive the electrospray, which is connected to an electrometer to read the current and then converted to a voltage read by the Arduino UNO. Pressure is measured in the vial and voltage is measured from the power source, although an oscilloscope was used to visualize the voltage trends, as shown in Figure 7. The visualization of the voltage allowed for a better understanding of how the PID loop within the angle-detection program was correcting for the voltage, and expedited the process of refining the PID gain values. The resulting PID loop, as shown in Figure 7, favored small incremental changes in voltage characterized by a gentle upward slope, minimizing any oscillation that may lead to the destabilization of the Taylor cone.

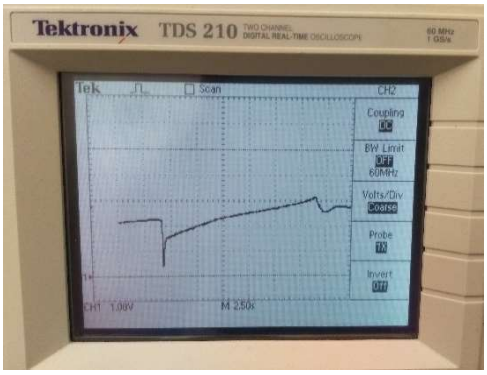

Figure 7. Screen capture of Tektronix TDS 210 oscilloscope output taken from phone video. An oscilloscope was used to visualize trends in voltage for a better representation of the PID loop's output. In this visualization, the oscilloscope displays the smooth rise in voltage as the PID loop within the angle-detection program attempts to correct for a disruption, characterized by the sharp drop in voltage near the left. Photo by author.

To determine the stability island of electrospray with ferrofluids, the relationship between minimum flow rate and magnetic field needed to be observed. In various magnetic fields, a spray using Ferrotec EFH1 ferrofluid was controlled over a range of cone angles with steps of 10 degrees, while pressure was steadily decreased. This gradual pressure loss was achieved with a large pressurized air tank that supplied air to the vial, which let out air through a small manually controlled valve as depicted in Figure 3. Pressure was converted to flow rate through Equation 2, the Hagen-Poiseuille equation, where pressure was measured in [kPa], viscosity in [mPa-s], capillary length in [cm], and capillary radius in [μm].

$$\Delta P = \frac{8\mu L Q}{\pi r^4} \qquad (2)$$

Starting at a flow rate of approximately 186.5 nL/s, air pressure was released from the vial in a steady way such that the ferrofluid flow rate was reduced at a rate of 5.3 nL/s^2, while the PID loop maintained the cone angle until the spray destabilized. Cone destabilization was characterized by a sharp drop in current and a rapid deviation in the cone angle from the set point. This was performed for cone angles ranging from 30 degrees to 80 degrees at intervals of

10 degrees, in magnetic fields of 356 gauss, 393 gauss, 2 gauss, -342 gauss, and with no magnet. The magnetic field was controlled by adjusting the distance *z* between the tip of the capillary and a ring magnet behind it, calculated with the K&J Magnetics field calculator (n.d.) that utilizes the Biot-Savart model of permanent ring magnets shown in Equation 3:

$$B = \frac{B_r}{2}\left[\frac{D+z}{\sqrt{R_a^2+(D+z)^2}} - \frac{z}{\sqrt{R_a^2+z^2}} - \left(\frac{D+z}{\sqrt{R_i^2+(D+z)^2}} - \frac{z}{\sqrt{R_i^2+z^2}}\right)\right] \quad (3)$$

In the equation, *z* corresponds to the distance *z* previously depicted in Figure 3. B_r is the remanence field, or essentially the magnetic field strength of the permanent magnet. *D* is the distance from a pole face on the symmetry axis, or equivalently the height of the magnet. R_a is the outer radius of the magnet, while R_i is the inner radius of the magnet, as shown in Figure 8. Text data containing values for the tip angle, cone angle, output V from the program, pressure, measured voltage from the HV source, current, 12 bit output from the Arduino UNO, measured voltage from the Arduino UNO, PID value, set point, and position of the cone angle base were written line by line for each iteration of the angle detection loop, to produce text data in columns that was easily converted into spreadsheets. Spreadsheet data was then analyzed to observe the effects of varying a magnetic field on a magnetoelectrospray on the minimum flow rate, Q_{min}.

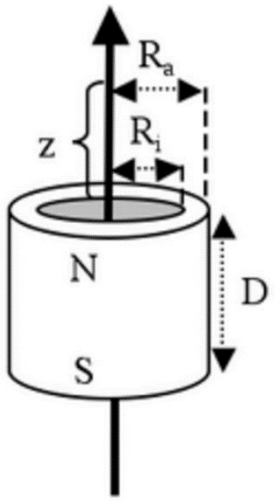

Figure 8. Ring magnet magnetic field. The magnetic field produced by a ring magnet can be calculated using the variables shown. Graphic from https://www.supermagnete.de/eng/faq/How-do-you-calculate-the-magnetic-flux-density#ring-magnet.

Data Curation

Between trials of different angles, the angle detection program would continue to print out measured values that would not be relevant in post-test analysis. Therefore, a data curation program was written in Python 2.7 and used to extract only the data where the measured angle and the set point had a difference less than 5% of the set point, and when the set point was a multiple of 10. This removes much of the irrelevant data during the period while pressure was replenished, producing cleaner spreadsheet data.

Results and Discussion

Angle-Detection

As the main goal of this experiment, the cone angle of the Taylor cone was successfully measured in real time. Accuracy was confirmed by referencing angle measurements from the angle-detection program to angles previously measured using a protractor. Multiple trials using both dark ferrofluid and clear hexane show that the angle-detection is robust enough for a variety of liquids, although the contrast between the background and the cone must be high and the background void of shadows or noise. The cone angle trackbar implementation for varying the angle base, the vertical line used in angle-detection, was also successful, allowing the user to adjust the base of the angle according to the capillary position relative to the frame in real time.

For normal electrosprays, where the Taylor cone does not bulge outwards at the tip of the capillary, the angle measurement is relatively accurate since the concave sides allow for externally tangent vectors to be drawn from the vertex to a certain point on the contour, previously depicted in Figure 4. However, magnetoelectrosprays are unique in that the Taylor cone bulges at the tip of the capillary due to magnetic forces, creating convex sides as shown in Figure 9 that are difficult for the angle-detection algorithm to draw externally tangent vectors at the cone tip. Nonetheless, with careful adjustment of the angle base, fairly precise angle measurements can still be achieved, as shown in Figure 9a. This problem is more noticeable for Taylor cones with an elongated curvature as shown in Figure 9d. The vectors that form the angle do not follow the contour tangentially; rather, the vectors cut through as secants, returning a measured angle at least 5 to 10 degrees smaller than expected. The same problem is similarly prevalent when the Taylor cone-jet is not parallel to the capillary, as shown in Figure 9b and Figure 9c. Generally, as the angle vector lengths increase, the error between the measured and expected angles becomes more noticeable, possibly up to differences of 15 to 20 degrees. However, this measuring error can be minimized by adjusting the cone base closer to the vertex of the Taylor cone. The tip angle, measured for scientific interest, was met with similar success as did the cone angle. Inaccuracy generally seems to stem from the single problem of convex cones, which is absent in the majority of regular electrosprays. Therefore, the angle-detection program is concluded to be viable and accurate for the angle-detection of Taylor cones in normal electrosprays, while still functional in magnetoelectrosprays despite sources of measuring error.

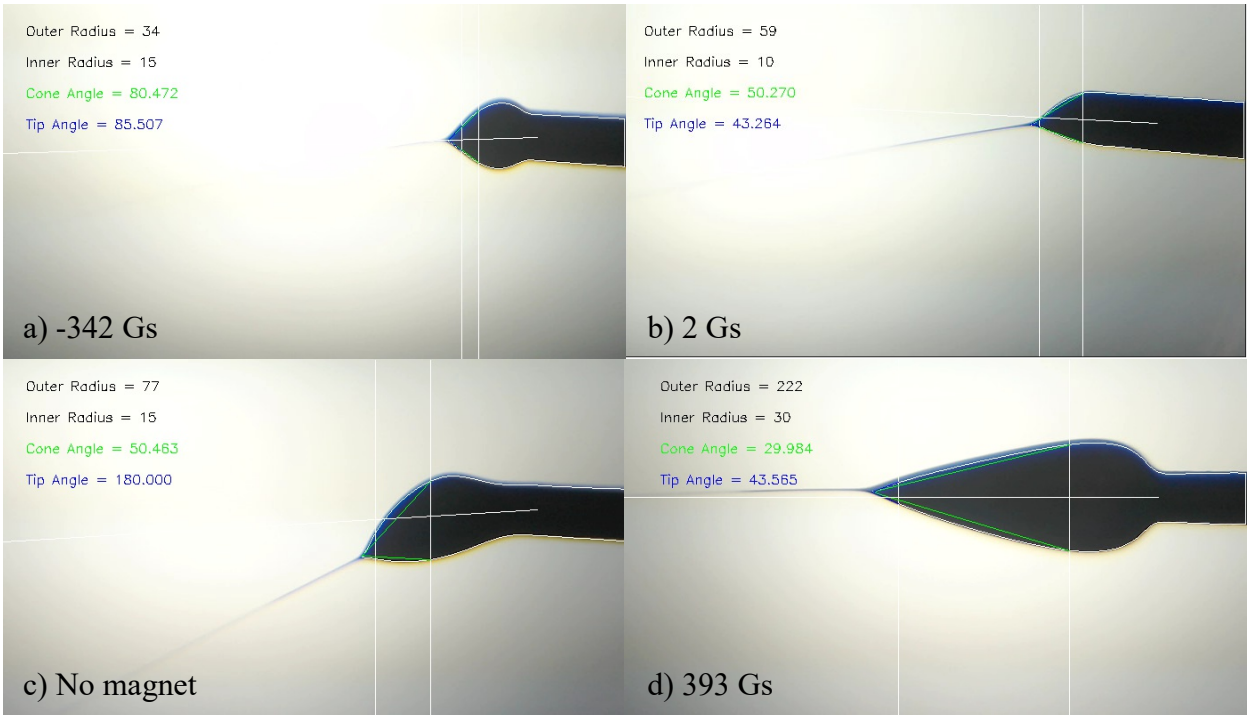

Figure 9. Angle-detection frames. The angle-detection program worked for cone stabilization in multiple magnetic fields, where (a) was controlled for 80° at -342 Gs, (b) was controlled for 50° at 2 Gs, (c) was controlled for 50° with no magnet, and (d) was controlled for 30° at 393 Gs. The right and left vertical lines correspond to the distance between the vertex and the cone angle base and the set distance of the tip angle base. In (a), the angle measured is fairly accurate as the vectors formed between the vertex and the cone angle base follow the cone outline, whereas in (b) and (c), the vectors cut through the inside of the cone as a result of the downward slant, resulting in a smaller measured angle than expected. In (d), the same thing occurs, but instead as a result of the elongated convex curvature of the cone. As the angle vector lengths increase from (a) to (d), the error between the expected and measured angles becomes more noticeable. Graphic by author.

PID Control

The PID loop with P, I, and D gain values of 0.0008, 0.0, and 0.8, respectively, was able to control for the set point, which in this case was the desired angle. Initial stabilization of a cone from an unstable stream was slow, since the low P gain value of 0.0008 resulted in a very gradual increases in voltage until reaching the critical voltage of the ferrofluid at which a cone-jet is ejected. However, once a cone was achieved and stabilized, the PID loop was able to maintain stability for extended periods of time of up to several hours, as well as quickly correct for small changes in cone angle in order to maintain the set point with a maximum stabilizing error - the difference between the measured angle and the set point - of ±2 degrees. A set point trackbar, similar to the one for the cone angle base, was implemented to allow for the adjustment of the set point in real time and therefore allowing the stabilization of various angles in one

instance of the program. With the ability to not only measure the angle of a Taylor cone, but also to stabilize the angle with relatively little stabilizing error, the angle-detection program was concluded to be overall successful.

Data Collection

With the angle-detection program and Arduino UNO interface functioning, the cone angle was controlled over a range of decreasing flow rates for the goal of widening the (Q,V) stability window towards lower flow rates. Six datasets were produced scanning pressure and cone angle at various magnetic fields. The trials at 123 gauss were repeated 3 times, trials at 2 gauss, -342 gauss, and with no magnet were repeated 2 times each, and trials at 393 gauss and 356 gauss were performed only once. During each trial, pressure, and in turn Q, was gradually lowered until the Taylor cone collapsed. Repeats minimize the effect of any possible errors and disturbances during each trial as the large number of controlled variables inevitably will cause some deviation between trials. The data was curated and compiled into one spreadsheet for each magnetic field, from which various relationships were analyzed for possible trends. As shown in Figure 10, the minimum flow rate versus magnetic field plot does not have enough data points to

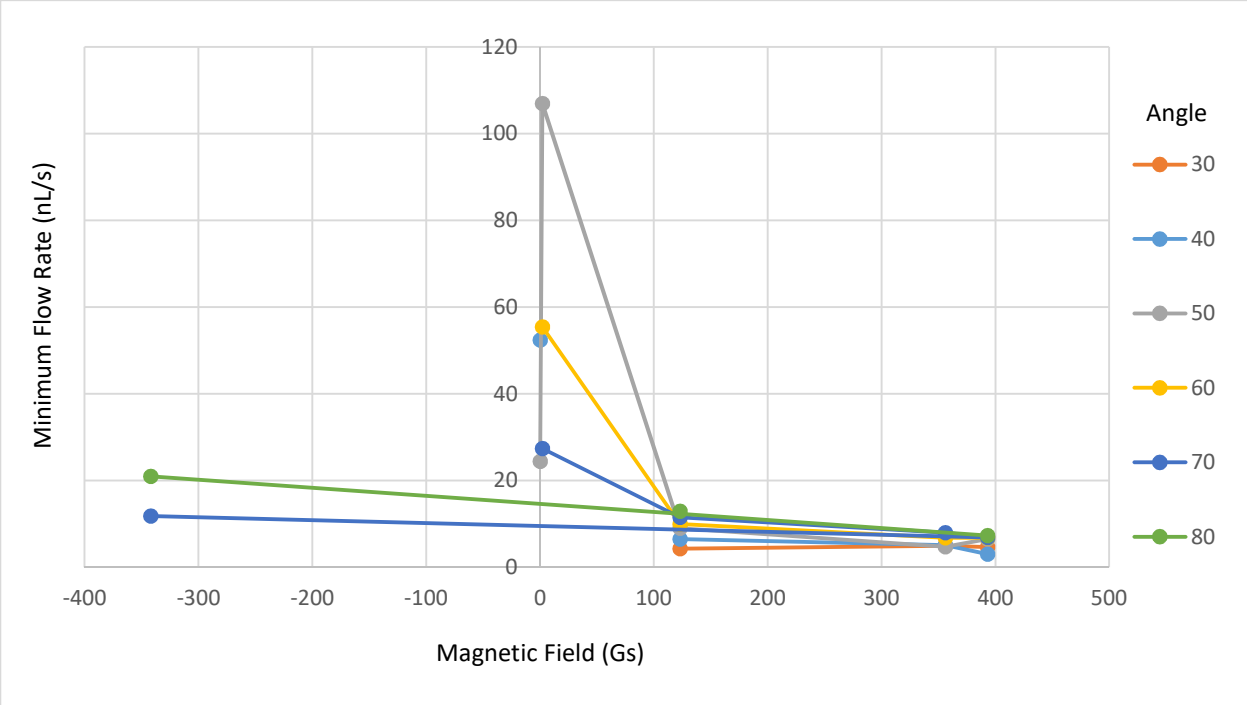

Figure 10. Minimum flow rate vs. magnetic field - initial data collected by author. The minimum flow rate versus magnetic field does suggest that flow rate tends to converge on lower values towards higher positive magnetic fields. The intervals at which the magnetic fields were increased could have been more consistent, as the trials at 0 and 2 Gs were essentially the same, while large gaps are apparent between trials of 2 and 123 Gs, 123 and 356 Gs. Negative magnetic fields were tested, but concluded to not be significant to the trends shown. Graphic by author.

convincingly show a general trend. However, in positive magnetic fields, the points do suggest that flow rate tends to converge towards lower values at higher magnetic fields. Negative magnetic fields were tested, but were concluded to not be significant in the trends shown. Therefore, further data was collected by an undergraduate student using a similar methodology based on the same angle-detection program and Arduino UNO setup developed by the author, at only positive magnetic fields of 97, 100, 200, 201, 300, 343, 350, and 393 gauss. Data was organized by the undergraduate student into spreadsheets and analyzed by the author for possible relationships between variables for insights on how magnetic field contributes to the stability of magnetoelectrosprays. The most relevant relationships for the goal of increasing the stability window and observing the extent of the stabilizing effect of a magnetic field on a magnetoelectrospray are Q_{min} versus magnetic field and Q_{min} versus V. Q_{min}, measured for each angle between 30° and 80° at intervals of 10°, was graphed against increasing magnetic fields to observe the its effect. As shown in Figure 11, there is a noticeable trend showing lower flow rates achieved as magnetic field increases for all angles, further supporting the hypothesis that a coincident magnetic field increases the stability of a magnetoelectrospray.

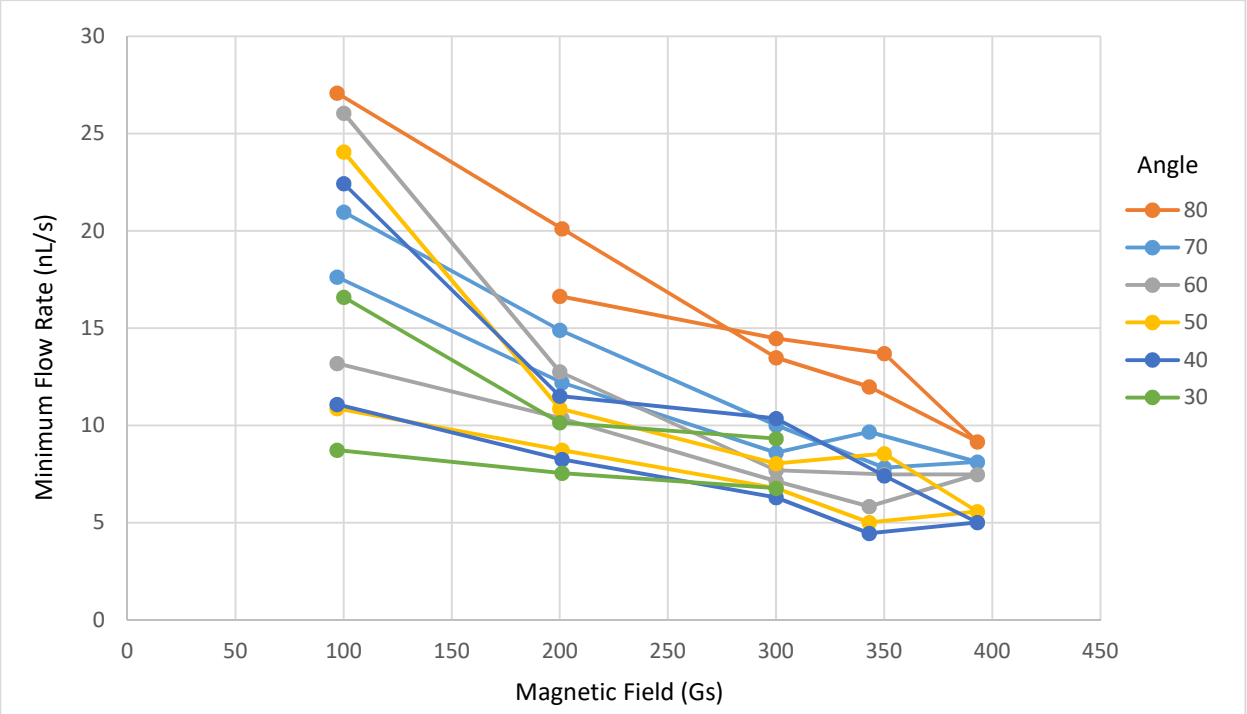

Figure 11. Minimum flow rate versus magnetic field with data collected by undergraduate student using the same Taylor cone stabilization setup developed by the author. Minimum flow rate at each angle was plotted against only positive magnetic fields, showing a noticeable trend between increasing magnetic field and lower flow rates. The hypothesis that flow rates tend to converge on lower values towards higher magnetic fields is further supported, with more consistent intervals of magnetic fields to provide a better characterization of the relationship between flow rate and magnetic field. Graphic by author.

This increased stability can also be observed on the Q_{min} versus V plane on which the stability window exists, as shown in Figure 12. The higher density of points towards the lower left corner of the stability window corresponds to the convergence of data points towards higher magnetic fields in Figure 11. Although there was no stability window for a non-magnetic electrospray with which the stability window of the magnetoelectrospray could be compared, the fact that the data congregates towards lower flow rates and lower voltages in the bottom-left corner of the stability window in conjunction with the trend between Q_{min} and B further suggests the comparable impact towards increased stability by a coincident magnetic field.

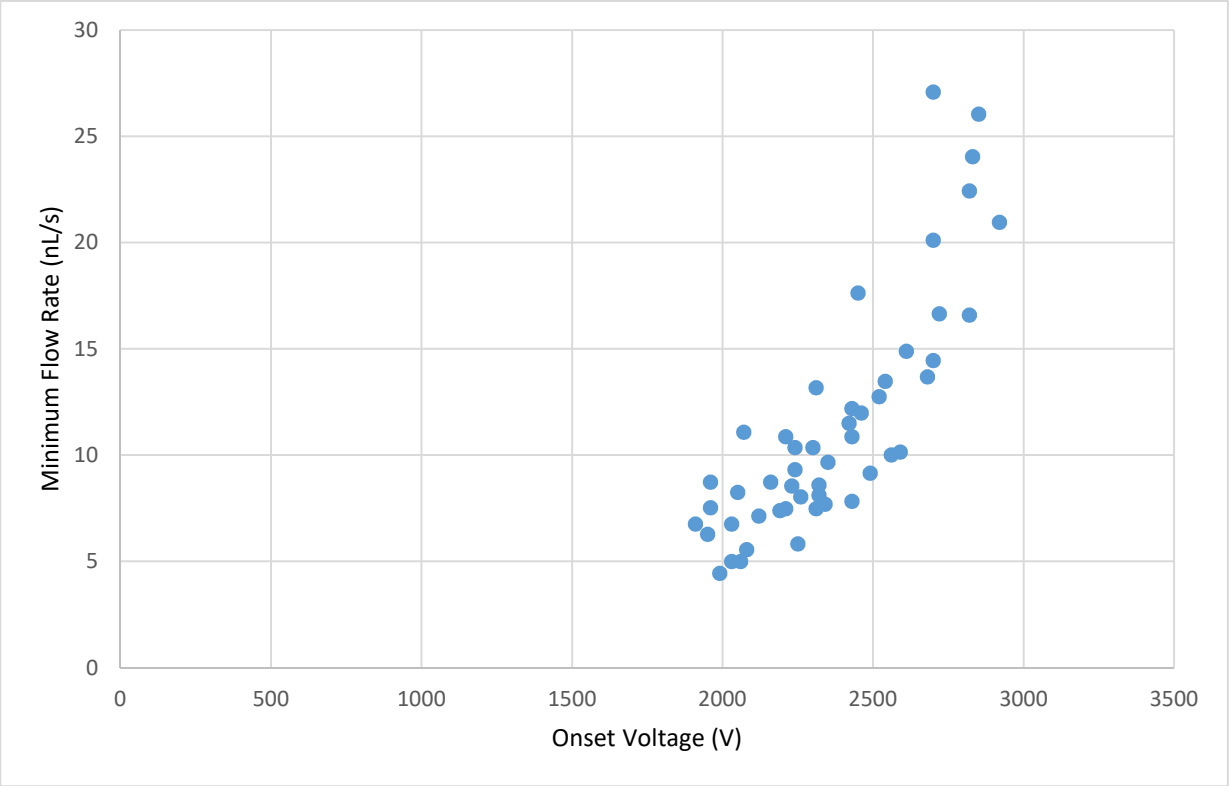

Figure 12. Minimum flow rate versus onset voltage with data collected by undergraduate student using the system developed by the author. The general shape that the data points form displays the lower-left bound of the (Q,V) stability window of the magnetoelectrospray, towards which most of the data is congregated. The high density of points towards the lower left of the shape corresponds to the converging points towards lower flow rates in Figure 11, and therefore it can be concluded that increasing magnetic fields may be important in expanding the stability window towards lower flow rates and voltages. Graphic by author.

Future Research

There were a few sources of error that may have led to inaccurate results, such as from the manual adjustment of the magnetic field and from the limited data that was collected. A follow-up study should repeat this methodology with a method of measuring the magnetic field more precisely than traditional manual methods such as using a caliper to measure the distance z between the emitter tip and the ring magnet. A method to measure the convex Taylor cones of a magnetoelectrospray with a much smaller measuring error should also be developed and implemented. With these improvements, this more precise methodology should then be repeated for many more magnetic fields in order to produce a higher resolution representation of the (Q,V) stability window. The development of a program that controls for the angle formed at the tip of a Taylor cone is of practical use in the future research of electrospray, since geometry becomes an easily controlled variable. With a method to automatically stabilize the cone angle, the unexplored area of study observing the effects of cone angle and shape on the resulting spray can be much more easily researched. If further research produces results that suggest a correlation between the cone angle and characteristics of the resultant electrospray, such as particle density, particle size, particle shape, or spray size and shape, then the cone angle becomes a significant controlling factor for electrosprays. The knowledge of how a locked angle affects the cone-jet can potentially also be used to improve medical devices, where the electrospray jet stream characteristics are important in the analysis of proteins and other biological particles through differential mobility analysis mass spectrometry or time-of-flight mass spectrometry. In relation to the expansion of the (Q,V) stability window, the increase in stability is ultimately in the hopes for the creation of a magnetoelectrospray in which multiple cone-jets are formed from Rosensweig instability-induced magnetic tips on one emitter, where the density and number of the cone-jets can be adjusted. Such a setup would allow for more efficient and stronger colloid thrusters that are much more precisely controlled.

Literature Cited

Astrom, K.J. (2002). PID control. *Control System Design*, 216-251.

Breslouer, O. (2010). Rayleigh-Plateau instability: falling jet.

Chen, C.H. (2011). Electrohydrodynamic stability. *Electrokinetics and Electrohydrodynamics in Microsystems* (Ed. A. Ramos), Springer, pp. 177-220.

Cloupeau, M., Prunet-Foch, B. (1989). Electrostatic spraying of liquids in cone-jet mode. *Journal of Electrostatics*, 22(2), 135-159.

Courtney, D.G., Dandavino, S., & Shea, H. (2002). Performance and applications of ionic electrospray micro-propulsion prototypes. *AIAA Space 2015-2222013.*

Durmusoglu, C. (2010). Discrete PID controller. Retrieved from http://code.activestate.com/recipes/577231-discrete-pid-controller/

Fernandez de la Mora, J. (2007). The fluid dynamics of Taylor cones. *Annual Review of Fluid Dynamics 2007*, 39, 217-243.

Hardy, C. (2014). The basics of tuning PID loops. Retrieved from http://innovativecontrols.com/blog/basics-tuning-pid-loops

Ho, C.S., Lam, C.W.K., Chan, M.H.M., Cheung, R.C.K., Law, L.K., Lit, L.C.W., Ng, K.F., Suen, M.W.M., & Tai, H.L. (2003). Electrospray ionisation mass spectrometry: principles and clinical applications. *Clinical Biochemist Reviews*, 24(1), 3-12.

K&J Magnetics Field Calculator [Computer Software]. Retrieved from https://www.kjmagnetics.com/fieldcalculator.asp

King, L.B., Meyer, E., Hopkins, M.A., Hawkett, B.S., & Jain, N. (2006). Self-assembling array of magnetoelectrostatic jets from the surface of a superparamagnetic ionic liquid. *Langmuir*, 2014, 30(47), 14143-14150.

Lenguito, G., Fernandez de la Mora, J., & Gomez, A. (2010). Multiplexed electrospray for space propulsion applications. *AIAA 2012-6521.*

Martinez-Sanchez, M. & Lozano, P. (2015). Cone-jet electrosprays, or colloid thrusters from MIT OpenCourseWare. Retrieved August 29, 2016, from http://ocw.mit.edu/courses/aeronautics-and-astronautics/16-522-space-propulsion-spring-2015/lecture-notes/

Roy, T., Hruby, V., Rosenblad, N., Rostler, P., & Spence, D. (2009). Cubesat propulsion using electrospray thrusters. *23rd Annual AIAA/USU Conference on Small Satellites*, 2009. SSC09-II-6.

Taylor, G. (1964). Disintegration of water drops in an electric field. *Proceedings of the Royal Society A*, 1964, 280(1382), 383-397.